Journal of ELECTRONIC MATERIALS, Vol. 36, No. 4, 2007
DOI: 10.1007/s11664-006-0083-3
© 2007 TMS
Special Issue Paper

Characterization of Epitaxial Indium Nitride Interlayers for Ohmic Contacts to Silicon Carbide

F.A. MOHAMMAD,[1] Y. CAO,[1] L.M. PORTER[1,2]

1.—Department of Materials Science and Engineering, Carnegie Mellon University, Pittsburgh, PA 15213, USA. 2.—E-mail: lporter@andrew.cma.edu

Ohmic contacts to *n*-type 4H- and 6H-SiC without postdeposition annealing were achieved using an interlayer of epitaxial InN beneath a layer of Ti. The InN films were grown by reactive dc magnetron sputtering at 450°C, whereas the Ti films were deposited by electron-beam evaporation at room temperature. The InN films were characterized by x-ray diffraction (XRD), secondary electron microscopy (SEM), cross-sectional transmission electron microscopy (TEM), and Hall-effect measurements. Both XRD and TEM observations revealed that the Ti and InN films have epitaxial relationships with the 6H-SiC substrate as follows: $(0001)[11\bar{2}0]_{Ti}||(0001)[11\bar{2}0]_{InN}||(0001)[11\bar{2}0]_{6H\text{-}SiC}$. The Ti/InN/SiC contacts displayed ohmic behavior, whereas Ti/SiC contacts (without an InN interlayer) were nonohmic. These results suggest that InN reduces the Schottky barrier height at the SiC surface *via* a small conduction-band offset and support previous reports of an electron accumulation layer at the surface of InN.

Key words: Ohmic contacts, silicon carbide (SiC), Schottky barrier height, epitaxy

INTRODUCTION

Silicon carbide (SiC) is a semiconductor being developed for high-temperature,[1] high-frequency,[2] and high-power[3] electronic devices because of its wide band gap, high breakdown voltage, and high thermal conductivity.[4] The fact that both *n*- and *p*-type single-crystal SiC wafers are commercially produced is a critical advantage for commercial development. However, ohmic contacts to SiC still do not have some of the desired properties for commercial applications. Specifically, the contacts often lack reproducible and consistent electrical properties, require high-temperature processing, and suffer from poor morphology.

Ohmic contacts to *n*-type SiC are typically formed by annealing Ni at temperatures above 900°C. Although Ni-based ohmic contacts have low specific contact resistance, the high-temperature postdeposition annealing step is undesirable because the reaction between Ni and SiC leads to broadening of the Ni-SiC interface, interface or surface roughening, formation of Kirkendall voids, or carbon segregation at the interface and throughout the metal layer.[5–11] These features inhibit long-term reliability and ultimately can cause device failure via contact degradation or wire bond failure,[12] an effect that is pronounced for smaller contact dimensions.

When reactions at the metal-semiconductor interface are prevented (i.e., by low-temperature processing), the contacts are referred to as nonalloyed contacts. Ohmic contacts formed without postdeposition annealing have been reported for semiconductors such as GaAs[13] and InAs,[14] InP,[14] ZnSe,[15] and GaN[16] by using suitable compositions and thicknesses of interlayer(s), or layer(s) in between the semiconductor and the primary metal contact layer. For example, a highly doped, narrow-band-gap $In_xGa_{1-x}As$ layer has been widely used as an interlayer for ohmic contacts to GaAs.[13] Because $In_xGa_{1-x}As$ has a smaller band gap (0.75 eV for $x = 0.5$) than GaAs (1.42 eV), an $InGa_{1-x}As$ interlayer can reduce the effective contact potential barrier and, therefore, the contact resistance.[13] An $In_xGa_{1-x}As$ interlayer is ideally suited for an ohmic

(Received July 19, 2006; accepted November 3, 2006; Published online February 16, 2007)

contact to GaAs, because its composition can be tailored to obtain the desired values of bandgap and work function. Moreover, InGaAs can be grown as an epitaxial layer on GaAs.

Indium nitride also has been reported to form an ohmic contact without annealing to GaAs[17] and to the metals Ti, Al, Ni, and Hg.[18] According to recent measurements,[19–21] InN films prepared using various processes are believed to contain a surface charge accumulation layer. This condition is expected to facilitate ohmic contact formation to a wide range of materials, as occurs in the semiconductors InAs and InSb.[22]

In this study, we report on InN as an ohmic interlayer between Ti and n-type SiC without postdeposition annealing. Because of the wide use of sputter deposition processes for the deposition of contacts and the prior use of sputter deposition to grow epitaxial InN films on various substrates,[23–25] we used sputtering to deposit the InN films in this study.

EXPERIMENTAL

All of the contact measurements were performed using nitrogen-doped n-type, single crystalline 4H- and 6H-SiC substrates manufactured by Cree Research Inc. (Durham, NC). The substrates were off-cut 8° and 3.5°, respectively, from the (0001) Si-terminated surface and contained the following additional specifications.

Substrate 1: N-doped, n-type (6.5×10^{18} cm^{-3}) homoepitaxial layer (epi thickness: 1 μm) on 0.04 Ω-cm, n-type *6H*-SiC; used for initial, qualitative I-V measurements.

Substrate 2: N-doped, n-type (9.8×10^{18} cm^{-3}) homoepitaxial layer (epi thickness: 1.5 μm) on N-doped, n-type (1.5×10^{17} cm^{-3}) homoepitaxial layer (epi thickness: 0.25 μm) on a 0.018 Ω-cm, n-type *4H*-SiC (0001) Si-face wafer; used for both initial, qualitative I-V measurements and specific contact resistance measurements.

An Al-doped, p-type 6H-SiC (0001) on-axis substrate without a homoepitaxial layer was used for the x-ray diffraction (XRD) and transmission electron microscopy (TEM) characterizations and Hall measurements of the InN films.

Each SiC surface was prepared for deposition by applying an RCA clean followed by wet oxidation at 1,100°C for 1 h and then etching the oxide in 10% HF for 5 min. The substrate was loaded into the sputtering system, which had a base pressure $<1 \times 10^{-8}$ torr, and annealed at 550°C for 10 min to desorb hydrocarbon contamination from the substrate surface. Prior to the deposition, the target was presputtered for 3 min to remove surface contaminants from the target surface.

Indium was sputtered from a 99.9999% pure In target in ultrahigh-purity nitrogen gas at a pressure of 10 mtorr. A dc magnetron sputtering source was used at a constant current of 0.05 amps, resulting in a deposition rate of 2.5 nm/min. The final thickness of the InN was 150 nm. The SiC substrate was maintained at a temperature of 450°C during the deposition.

Titanium was deposited in the same vacuum system using electron-beam evaporation at a deposition rate of ~10 nm/min onto unheated samples. The final thickness of the Ti was 100 nm.

A panalytical X'Pert PRO Diffractometer (Almelo, The Netherlands) was used to determine the crystalline properties of the film. The interface microstructure was analyzed by cross-sectional TEM using a JEM-2000EX (JEOL Tokyo, Japan) microscope.

The electrical characteristics of the InN films were determined from Hall-effect measurements at room temperature, at a voltage of 1 V and a magnetic field of 5,000 gauss. Current-voltage (I-V) measurements were performed at room temperature using an HP 4155B semiconductor parameter analyzer (Agilent Technologies, Englewood, CO) and a Signatone (Lucas Signatone Corp. Gilroy, CA) S-1,060H-4QR high-temperature probe. For estimation of the specific contact resistance, contacts on substrate 2 were photolithographically patterned using a mask consisting of 300 × 50 μm rectangular pads in accordance with the transfer length method (TLM). The spacings between the pads were 5 μm, 10 μm, 20 μm, 30 μm, and 50 μm, respectively. The Ti and the InN layers were etched using Ar ion milling. Due to technical difficulties, mesa isolation around the contact sets was not performed; thus, there may be an appreciable current flow around the contact pads, reducing the accuracy of the experimentally determined specific contact resistance. However, because the contacts were not alloyed, the sheet resistance values underneath the contact pads and in the semiconductor film should be equivalent, thus avoiding a major source of error arising from unequal sheet resistivities,[26] which are typical in alloyed contacts. In consideration of the described conditions, the specific contact resistance value is reported as a preliminary estimate.

RESULTS

Materials Characterization

An XRD θ-2θ scan of the Ti/InN/6H-SiC structure is shown in Fig. 1a; the sample is oriented such that the {0006} planes in SiC satisfy the Bragg diffraction condition. The only other diffraction peaks observed are from the {0002} planes in InN and Ti. These results show that there is an orientation relationship among the three layers: $\{0001\}_{\mathrm{Ti}} || \{0001\}_{\mathrm{InN}} || \{0001\}_{\mathrm{6H\text{-}SiC}}$.

The in-plane orientations of the Ti and the InN films were determined by performing azimuthal ϕ-scans and by comparing the locations of the $\{10\bar{1}1\}$Ti, $\{10\bar{1}1\}$InN, and $\{10\bar{1}1\}$6H-SiC diffraction peaks in ϕ-space (ϕ is the angle of rotation). The three ϕ-scans are overlaid in Fig. 1b, although it should be emphasized that they were acquired at

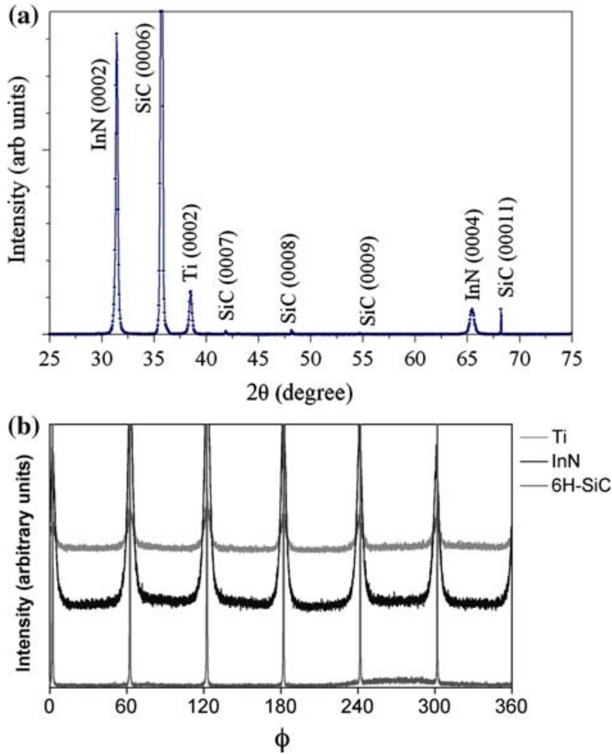

Fig. 1. XRD patterns of Ti/InN/6H-SiC(0001): (a) θ-2θ scan [θ = 0° and ψ = 0°] and (b) azimuthal off-axis ϕ scans of the {10$\bar{1}$1} reflections for Ti [2θ = 40.18° and ψ = 61.37°], InN [2θ = 33.24° and ψ = 61.74°], and 6H-SiC [2θ = 34.12° and ψ = 79.99°].

different 2θ and ψ (the sample tilt) angles (2θ = 40.18°, ψ = 61.37° for {10$\bar{1}$1}Ti; 2θ = 33.24°, ψ = 61.74° for {10$\bar{1}$1}InN; and 2θ = 34.12°, ψ = 79.99° for {10$\bar{1}$1}6H-SiC). The hexagonal symmetry of the Ti, InN, and 6H-SiC crystal lattices dictates that there are six planes in the {10$\bar{1}$1} family. As shown in Fig. 1b, six diffraction peaks for SiC, six for InN, and six for Ti were obtained from the 360° ϕ-scans; each of these reflections is from one member in the {10$\bar{1}$1} family of planes. This result indicates that the Ti and the InN films have only one in-plane orientation (texture). Furthermore, the reflections from {10$\bar{1}$1}Ti, {10$\bar{1}$1}InN, and {10$\bar{1}$1}6H-SiC are parallel to each other. Therefore, the following orientation relationship in the basal plane can be written as $[11\bar{2}0]_{Ti}||[11\bar{2}0]_{InN}||[11\bar{2}0]_{6H\text{-}SiC}$.

The full-width at half-maximum value of the XRD rocking curve was 1.4°, which indicates that the films contain many low-angle grain boundaries. The scanning electron microscopy (SEM) images (Fig. 2) showed continuous films with some surface roughness, attributed to the textured morphology.

Cross-sectional TEM was used to analyze the interfacial microstructure and to confirm the phase formation and epitaxial orientation of the Ti and InN layers. A cross-sectional TEM image of the interface is shown in Fig. 3a. The InN film is dense, columnar, and has a flat interface with the SiC. No voids were observed in the film.

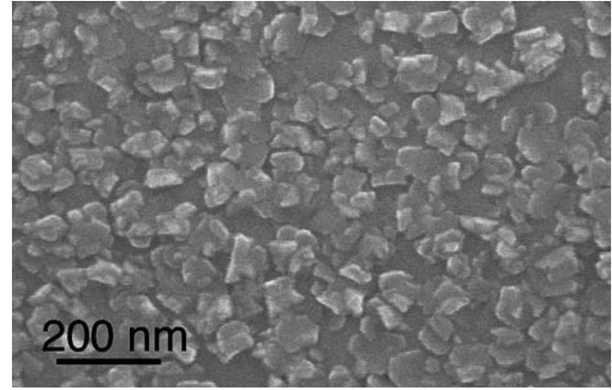

Fig. 2. SEM image of the surface of an InN film, which was reactively sputtered on SiC at 450°C.

The selected area diffraction patterns from the InN/6H-SiC (Fig. 3b) and the Ti/InN/6H-SiC (Fig. 3c) interfaces display aligned arrays of diffraction spots. The patterns confirm the epitaxial orientation relationships of the Ti and InN films with the 6H-SiC substrate: $(0001)_{Ti}||(0001)_{InN}||(0001)_{6H-SiC}$, and $[11\bar{2}0]_{Ti}||[11\bar{2}0]_{InN}||[11\bar{2}0]_{6H-SiC}$. These results are in agreement with the XRD results.

It was previously reported[27] that Ti grows epitaxially on 6H-SiC; there is a –4% lattice mismatch between $(1\bar{1}00)_{Ti}$ and $(1\bar{1}00)_{6H\text{-}SiC}$. The results of this work show that both the InN interlayer and the top Ti layer grew epitaxially on SiC even though the lattice mismatches are considerable (~16% between $(1\bar{1}00)_{InN}$ and $(1\bar{1}00)_{6H\text{-}SiC}$ and –17% between $(1\bar{1}00)_{Ti}$ and $(1\bar{1}00)_{InN}$).[28–30]

Figure 4 shows a high-resolution image of the InN/6H-SiC interface along the [11$\bar{2}$0]6H-SiC zone axis. Careful examination reveals that the initial few monolayers of InN are disordered, beyond which the layers are crystalline and oriented. The epitaxial relationship between the InN and the 6H-SiC is again confirmed from the fast fourier transform (FFT) pattern (shown in the inset of Fig. 4). Occasionally, polycrystalline grains of InN were found just beyond the interface. However, the primary structure of the films was oriented, as described in the paragraphs above.

Electrical Measurements

Hall measurements were used to quantify the carrier type, concentration, and mobility in the InN films. Titanium was used as the ohmic contacts. The films were found to be n-type with an electron concentration of 1×10^{20} cm^{-3} and a mobility of 140 cm^2/Vs. Although the carrier concentration (mobility) is higher (lower) than that in some thick (~100 nm) InN films produced by molecular beam epitaxy, these values are quite typical of the higher quality sputtered films. Furthermore, a high carrier concentration is actually beneficial for the purpose of making low-resistive ohmic contacts.

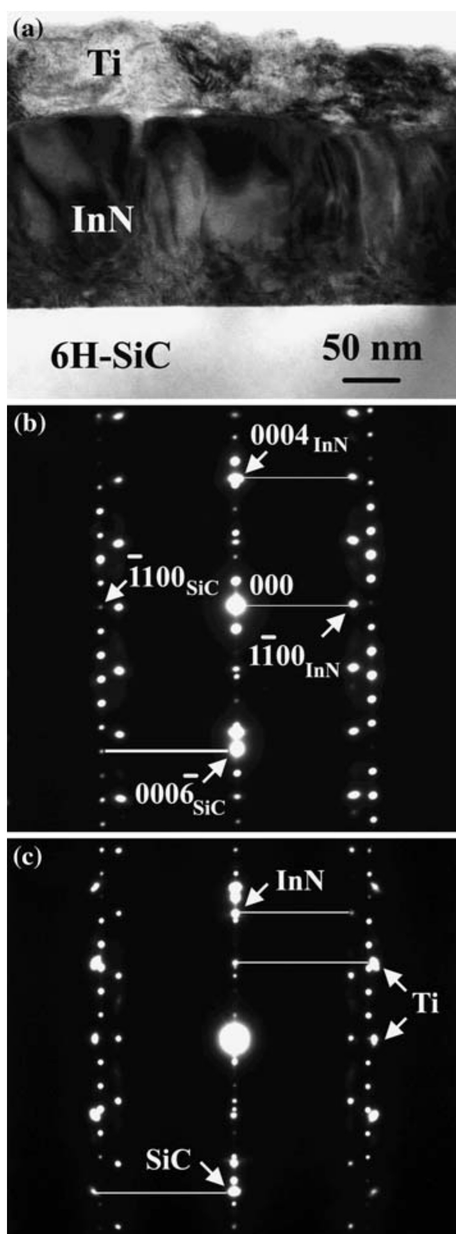

Fig. 3. (a) Cross-sectional TEM image of the Ti/InN/6H-SiC, (b) selected area diffraction (SAD) pattern from the InN/6H-SiC interface, and (c) SAD pattern from the Ti/InN/6H-SiC interface Ti, InN, and 6H-SiC have hexagonal crystal structures. z = [11$\bar{2}$0] in both (b) and (c).

The I-V measurements were performed to determine the electrical effect of the InN interlayer between Ti and n-type SiC. Figure 5 shows representative I-V characteristics of Ti(100 nm)/6H-SiC and Ti(100 nm)/InN(150 nm)/6H-SiC, both in the as-deposited condition. These measurements represent contacts having diameters of 500 μm and a center-to-center spacing of 1,000 μm. We found that the contacts without an InN interlayer were semi-ohmic and relatively resistive. In comparison, the contacts that contained an InN interlayer were ohmic and at least two orders of magnitude less resistive. Based on the TLM structures described in the "Experimental" section, a preliminary estimate of the specific contact resistance of Ti/InN/4H-SiC (sample 2) is $1.8 \times 10^{-4}\ \Omega\ \text{cm}^2$. The calculated value of sheet resistance (233 Ω/sq) is in good agreement with that expected for the doping concentration and thickness of the epilayer.[31]

Although the Ti contacts were deposited at room temperature, rather than at the 450°C deposition temperature of the InN films, our prior experience shows that much higher annealing temperatures (~700°C) are required to significantly affect the electrical characteristics of Ti on SiC.[32] The fabrication of ohmic contacts between transition metals and SiC requires annealing temperatures >900°C. Furthermore, the SiC surfaces were desorbed in ultrahigh vacuum immediately before the depositions, and the two deposition temperatures should not have significantly different effects on surface oxide content, because much higher temperatures are required to desorb SiO_2. Therefore, we attribute the difference in electrical behavior to the presence of the InN interlayer.

DISCUSSION

Our initial reasons for selecting InN as an interlayer contact to SiC can give us some insight into the possible mechanism(s) for ohmic behavior. In addition to considerations such as its small band gap (~0.8 eV)[33,34] and high n-type conductivity, we selected InN based on our preliminary estimate of the conduction-band offset between SiC and InN. Our estimate was based primarily on the following published values of the valence-band (ΔE_V) offsets: $\Delta E_v(\text{6H - SiC(0001)} - \text{AlN(0001)}) = 1.4 \pm 0.3$ eV[35] and $\Delta E_v(\text{GaN(0001)} - \text{AlN(0001)}) = 0.8 \pm 0.2$ eV[36].

Based on the band gaps (E_g) of these semiconductors, the conduction-band (ΔE_C) offsets can be calculated as follows: $\Delta E_c(\text{6H - SiC} - \text{AlN}) = E_g(\text{AlN}) - E_g(\text{6H - SiC}) - \Delta E_v = 6.2 - 3.0 - 1.4 = 1.8 \pm 0.3$ eV, and $\Delta E_c(\text{GaN} - \text{AlN}) = E_g(\text{AlN}) - E_g(\text{GaN}) - \Delta E_v = 6.2 - 3.4 - 0.8 = 2.0 \pm 0.2$ eV. Therefore, $\Delta E_c(6H - SiC - GaN) = \Delta E_c(6H - SiC - \text{AlN}) - \Delta E_c(G\text{aN} - \text{AlN}) = -0.2 \pm 0.5$eV.

Although we found no similar measurements for InN, Lin et al.[16] reported that n-type InN formed a nearly ohmic contact with n-type GaN. From this result, we deduced that the conduction-band offset between InN and GaN is small and, therefore, the conduction-band offset between InN and 6H-SiC should also be small, as calculated above for $\Delta E_C(\text{6H - SiC} - G a\text{N})$.

Although a small conduction-band offset between InN and SiC is indeed possible, more recent results indicate that another phenomenon also plays a critical role in the ohmic behavior. It was reported that Ti, Al, and Ni all formed ohmic contacts to InN without annealing.[18] From these results, along with spectroscopy measurements of various InN surfaces, it is believed that the InN surfaces have an

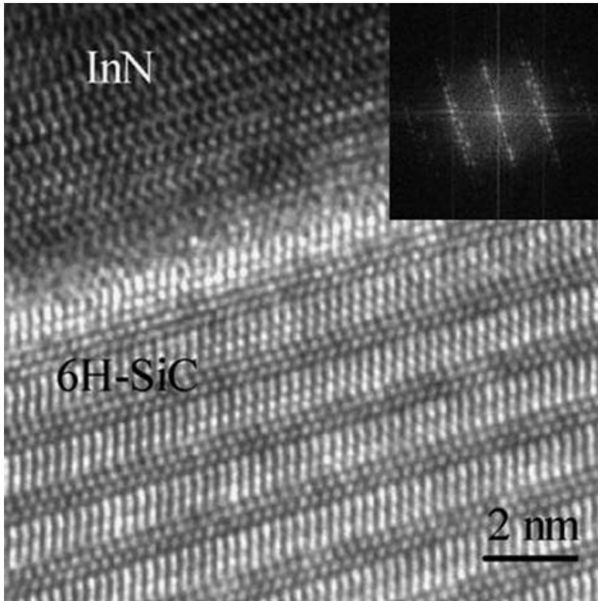

Fig. 4. High-resolution TEM image of the InN/6H-SiC interface and the corresponding FFT pattern (inset).

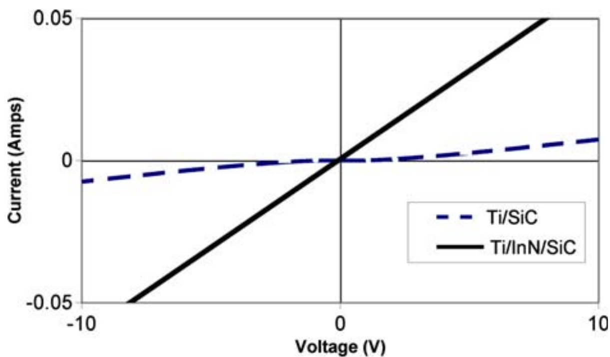

Fig. 5. I-V characteristics of Ti(100 nm)/6H-SiC and Ti(100 nm)/InN(150 nm)/6H-SiC. The 6H-SiC epilayer is doped n-type 6.5×10^{18} cm^{-3}.

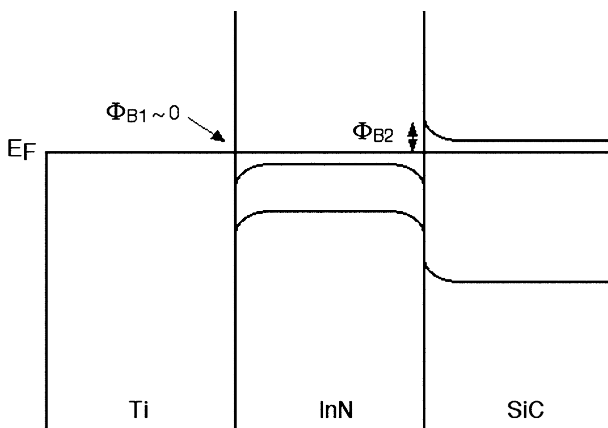

Fig. 6. Proposed energy band relationships for the Ti/InN/SiC contacts.

electron accumulation layer.[19–21] Thus, InN is expected to easily form ohmic contacts to a variety of materials in a manner similar to InAs.

A qualitative diagram of our proposed energy band relationship is illustrated in Fig. 6. As shown in the figure, the Schottky barrier height, Φ_{B1}, between the Ti and the InN interlayer is expected to be zero, due to an electron accumulation layer (downward band bending) at the surface of the InN and the high density of electronic states (zero band bending) in the Ti. The Schottky barrier height Φ_{B2}, between the InN and the SiC, is considered to exist only on the SiC side of the interface, again due to an accumulation layer at the InN surface. A small ΔE_C would be required to yield a sufficiently small Φ_{B2} at the SiC surface.

For the structure to be ohmic, both Φ_{B1} and Φ_{B2} should be sufficiently small or have a narrow space charge layer. For the Ti/InN/SiC contacts, we propose that the following conditions promote ohmic behavior.

- The InN and SiC have the same doping type.
- The high n-type carrier concentration of the InN interlayer enhances conductivity across the layer.
- The barrier height between the InN and Ti is effectively zero due to downward band bending in InN[21] and the high density of electronic states in the metal. (The relatively low work function of Ti[37] is generally helpful in forming ohmic contacts to n-type semiconductors, but may not be necessary in this case.)
- The barrier between the InN and SiC is reduced relative to the metal-SiC interfaces.

We also believe that the epitaxial quality of the InN films, as shown by the XRD and TEM results (Figs. 1–4), is important to the resulting electrical characteristics of the films and ultimately the ohmic behavior of the contacts.

CONCLUSIONS

In summary, epitaxial growth of Ti on InN on SiC by dc magnetron sputtering was observed using cross-sectional TEM and corresponding selected area diffraction patterns along with XRD; the samples were ohmic without postdeposition annealing. The ohmic behavior was proposed to be associated with an electron accumulation layer in the InN and a Schottky barrier-height reduction mechanism.

ACKNOWLEDGEMENTS

The authors gratefully acknowledge the research support from the National Science Foundation (Grant Nos. ECS-9875186 and DMR-0354939). The films in this study were grown using equipment funded by the National Science Foundation (Grant No. DMR-9802917). Valuable discussions with Dr. Kumar Das, Tuskegee University, are also greatly appreciated.

REFERENCES

1. M.A. Capano and R.J. Trew, *MRS Bull.* 22, 19 (1997).
2. R.J. Trew, J.-B. Yan, and P.M. Mock, *Proc. IEEE* 79, 598 (1991).
3. J.A. Cooper Jr., M.R. Melloch, R. Singh, A. Agarwal, and J.W. Palmour, *IEEE Trans. Electron. Dev.* 49, 658 (2002).
4. G.A. Slack, *J. Appl. Phys.* 35, 3460 (1964).
5. J. Crofton, P.G. McMullin, J.R. Williams, and M.J. Bozack, *J. Appl. Phys.* 77, 1317 (1995).
6. M.G. Rastegaeva, A.N. Andreev, and A.A. Petrov, *Mater. Sci. Eng. B* 46, 254 (1997).
7. A. Kakanakova-Georgieva, T. Marinova, and O. Noblanc, *Thin Solid Films* 343, 637 (1999).
8. S.Y. Han, J.Y. Shin, and B.T. Lee, *J. Vac. Sci. Technol. B* 20, 1496 (2002).
9. E. Kurimoto, H. Harima, and T. Toda, *J. Appl. Phys.* 91, 10215 (2002).
10. L.D. Madsen, E.B. Svedberg, H.H. Radamson, C. Hallin, and B.H. Jorvarsson, *Mater. Sci. Forum* 338, 981 (2000).
11. T. Marinova, R. Yakimova, and V. Krastev, *J. Vac. Sci. Technol. B* 14, 3252 (1996).
12. M.W. Cole, P.C. Joshi, and C.W. Hubbard, *J. Appl. Phys.* 88, 2652 (2000).
13. T.C. Shen, G.B. Gao, and H. Morkoc, *J. Vac. Sci. Technol. B* 10, 2113 (1992).
14. P.W. Leech and G.K. Reeves, *Mater. Res. Soc. Symp. Proc.* 318, 183 (1994).
15. R.G. Dandrea and C.B. Duke, *Appl. Phys. Lett.* 64, 2145 (1994).
16. M.E. Lin, F.Y. Huang, and H. Morkoc, *Appl. Phys. Lett.* 64, 2557 (1994).
17. C.R. Abernathy, S.J. Pearton, F. Ren, and P.W. Wisk, *J. Vac. Sci. Technol. B* 11, 179 (1993).
18. H. Lu, W.J. Schaff, L.F. Eastman, and C.E. Stutz, *Appl. Phys. Lett.* 82, 1736 (2003).
19. I. Mahboob, T.D. Veal, C.F. McConville, H. Lu, and W.J. Schaff, *Phys. Rev. Lett.* 92, 036804 (2004)–1.
20. K.A. Rickert, A.B. Ellis, F.J. Himpsel, H. Lu, W.J. Schaff, J.M. Redwing, F. Dwikusuma, and T.F. Kuech, *Appl. Phys. Lett.* 82, 3254 (2003).
21. T.D. Veal, I. Mahboob, L.F.J. Piper, C.F. McConville, H. Lu, and W.J. Schaff, *J. Vac. Sci. Technol. B* 22, 2175 (2004).
22. V.Y. Aristov, V.M. Zhilin, C. Grupp, A. Taleb-lbrahimi, H.J. Kim, P.S. Mangat, P. Soukiassian, and G. Le Lay, *Appl. Surf. Sci.* 166, 263 (2000).
23. Q.X. Guo, A. Okada, H. Kidera, T. Tanaka, M. Nishio, and H. Ogawa, *J. Cryst. Growth* 237, 1032 (2002).
24. T.J. Kistenmacher, S.A. Ecelberger, and W.A. Bryden, *J. Appl. Phys.* 74, 1684 (1993).
25. Z.G. Qian, W.Z. Shen, H. Ogawa, and Q.X. Guo, *J. Appl. Phys.* 92, 3683 (2002).
26. D.K. Schroder, *Semiconductor Material and Device Characterization,* 2nd edn. (New York: John Wiley & Sons, 1998). pp. 138–159.
27. L.M. Porter, R.F. Davis, J.S. Bow, M.J. Kim, and R.W. Carpenter, *J. Mater. Res.* 10, 668 (1995).
28. "Powder Diffraction File," compiled by the International Center for Diffraction Data, Newtown Square, PA, http://www.icdd.com, 1993.
29. C.Y. Yeh, Z.W. Lu, S. Froyen, and A. Zunger, *Phys. Rev. B* 46, 10086 (1992).
30. Tairov Y.M., Tsvetkov V.F., in *Progress in Crystal Growth and Characterization 7*, ed. P. Krishna (New York: Pergamon, 1983), pp. 111–143.
31. Cree Research, Durham, NC.
32. L.M. Porter, R.F. Davis, J.S. Bow, M.J. Kim, R.W. Carpenter, and R.C. Glass, *J. Mater. Res.* 10, 668 (1995).
33. T. Matsuoka, H. Okamoto, M. Nakao, H. Harima, and E. Kurimoto, *Appl. Phys. Lett.* 81, 1246 (2002).
34. J. Wu, W. Walukiewicz, K.M. Yu, J.W.A. III, E.E. Haller, H. Lu, W.J. Schaff, Y. Saito, and Y. Nanishi, *Appl. Phys. Lett.* 80, 3967 (2002).
35. S.W. King, R.F. Davis, C. Ronning, M.C. Benjamin, and R.J. Nemanich, *J. Appl. Phys.* 86, 4483 (1999).
36. S.W. King, C. Ronning, R.F. Davis, M.C. Benjamin, and R.J. Nemanich, *J. Appl. Phys.* 84, 2086 (1998).
37. *CRC Handbook of Chemistry and Physics*, 86th ed. (New York: CRC Press, 2005), p. 12-114.